Contents lists available at ScienceDirect

Translational Oncology

Original Research

Suppression of FAM83D Inhibits Glioma Proliferation, Invasion and Migration by Regulating the AKT/mTOR Signaling Pathway

Xia Li [1], Cui Sun [1], Jing Chen, Ji-Fen Ma, Yi-Heng Pan [*]

Center for Diagnosis and Treatment of Neuro-oncology Diseases, Taihe Hospital, Hubei University of Medicine, Shiyan 442000, Hubei, China

ARTICLE INFO

ABSTRACT

Objective: To explore the mechanism by which the family with sequence similarity 83, member D (FAM83D)-mediated AKT/mTOR signaling pathway activation affects the proliferation and metastasis of glioma cells.
Methods: FAM83D protein expression in glioma cells and tissues was detected by western blotting. Glioma U87 and U251 cells were selected and divided into the Mock, siNC, siFAM83D, FAM83D, MK2206 and FAM83D + MK2206 groups. Cell proliferation was assessed by MTT (3-[4,5-dimethylthiazol-2-yl]-2,5 diphenyl tetrazolium bromide) and clone formation assays, while invasion and migration were evaluated by Transwell assays and wound healing tests. The protein expression of members of the AKT/mTOR pathway was determined via western blotting. Xenograft models were also established in nude mice to observe the *in vivo* effect of FAM83D on the growth of glioma.
Results: FAM83D was upregulated in glioma patients, especially in those with Stage III-IV. In addition, cells treated with siFAM83D had significant downregulation of p-AKT/AKT and p-mTOR/mTOR, with decreased proliferation and colony numbers, as well as decreased invasion and migration compared to the Mock group. However, FAM83D overexpression could activate the Akt/mTOR pathway and promote the proliferation, invasion and migration of glioma cells. Moreover, treatment with MK2206, an inhibitor of AKT, reversed the promoting effect of FAM83D on the growth of glioma cells. The *in vivo* experiments demonstrated that silencing FAM83D could inhibit the *in vivo* growth of glioma cells
Conclusion: FAM83D was upregulated in glioma and silencing FAM83D suppressed the proliferation, invasion and migration of glioma cells via inhibition of the AKT/mTOR pathway.

Introduction

Brain glioma, a common tumor in the nervous system, accounts for nearly 80% of primary malignant tumors in the central nervous system (CNS) and is the leading cause of death of patients with intracranial tumors [1]. Glioma is characterized by aggressive invasion, rapid growth and an indistinct boundary, resulting in tremendous difficulties in radical resection [2,3]. Despite advances in the techniques of surgery, chemotherapy and radiotherapy in recent decades, patients still suffer from high rates of postoperative recurrence, a poor prognosis and a short survival time [4,5]. The median survival time of patients with adult glioblastoma multiforme (GBM) is only 14 months [6]. Brain glioma severely threatens the health of humans, causing tremendous pain and substantial social burdens [7]. Thus, a deep understanding of the genetic and molecular mechanisms involved in the progression of glioma is necessary to develop novel strategies for the diagnosis and treatment of glioma [8].

Family with sequence similarity 83, member D (FAM83D), as a member of the FAM83 (family with sequence similarity 83) family, is located at chromosome 20q, showing an association with tumor development [9]. Silencing FAM83D could downregulate the expression of FBXW7, a tumor suppressor gene, to induce apoptosis while inhibiting the proliferation and colony formation of breast cancer cells [9]. Additionally, knockout of FAM83D was demonstrated to inhibit the growth of colorectal cancerous cells by suppressing the FBXW7/Notch1 signaling pathway [10]. Together, these results indicate the possible involvement of FAM83D in the development and progression of various tumors. In this study, using recently available cancer genomic data from The Cancer Genome Atlas (TCGA), we found that the expression of FAM83D was dramatically increased in GBM patients. However, the

---

function and mechanism of FAM83D in glioma have not yet been studied. Thus, we explored the role of FAM83D in glioma in the present study.

Existing data suggest that the PI3K/AKT/mTOR axis is the major pathway involved in various biological processes, including proliferation, invasion and migration, thus playing pivotal roles in tumors [11, 12]. To date, increasing evidence indeed confirms the involvement of AKT/mTOR in the progression of glioma [13]. Notably, Yin C *et al.* revealed that FAM83D could accelerate the EMT, proliferation and invasion of non-small cell lung cancer (NSCLC) by activating AKT/mTOR [14]. Hence, we hypothesized that FAM83D could also be implicated in the development and progression of glioma by regulating the AKT/mTOR pathway.

Therefore, this study was designed to demonstrate the influence of FAM83D-mediated AKT/mTOR in glioma cells on proliferation and metastasis, which may provide novel insights for the treatment of glioma.

Materials and methods

Ethics statement

This study was approved by the Ethics Committee of our hospital, and all patients were informed of the content of this study and signed written informed consent forms prior to enrollment. The animal experiments were conducted according to the Guide for the Care and Use of Laboratory Animals issued by the National Research Council (US) Committee for the Update of the Guide for the Care and Use of Laboratory Animals [15] and approved by the Ethical Committee for Laboratory Animals of our hospital.

Subjects

Samples were collected from surgically resected brain glioma tissues that were confirmed by pathological examination and adjacent normal tissues from 67 patients between Jan 2017 and December 2020, including 39 men and 28 women aged between 38 and 71 years, with an average age of 44.9 ± 13.1 years. Prior to the surgery, patients had no history of chemotherapy, radiotherapy or immunotherapy. Glioma was classified into four grades based on the 2016 World Health Organization Classification of Tumors of the Central Nervous System [16], and there were 36 in Grades I-II and 31 in Grades III-IV among these patients.

Cell culture

The glioma cell lines (U87, U251, T98G, SHG44 and U118) and normal human astrocytes (NHAs) were provided by the Shanghai Institute of Biochemistry and Cell Biology, Chinese Academy of Sciences. They were maintained in Dulbecco's modified Eagle's medium (DMEM) (Thermo Fisher Scientific Inc., USA) with 10% fetal bovine serum (FBS) in an incubator at 37°C with 5% CO_2. The medium was refreshed every two days, and the cells were passaged when they reached 70% to 80% confluence. Cells in logarithmic phase were adopted for the following experiments.

Cell grouping and transfection

The glioma cell lines U87 and U251 were selected and divided into the Mock group, siNC group, siFAM83D group, FAM83D group, MK2206 group and FAM83D + MK2206 group. Cells in the Mock group received no treatments or transfection; those in the siNC group and siFAM83D group were transfected with negative control siRNA and FAM83D siRNA, respectively. Cells in the FAM83D group were transfected with the pcDNA3.1-FAM83D plasmid, and cells in the MK2206 group were treated with 8 μM AKT inhibitor MK2206 (Beyotime, Jiang Su, China) for 24 h [14]. Cells in the FAM83D + MK2206 group were transfected

with the pcDNA3.1-FAM83D plasmid and then treated with MK2206 for 24 h.

Glioma cells in logarithmic growth phase were digested with trypsin, counted and seeded in a 6-well plate at a density of 1×10^6 cells/well for growth, and when the cell confluence reached approximately 70%-80%, transfection was carried out as per the instructions of Lipofectamine™ 2000 (Invitrogen, USA). Negative control siRNA, FAM83D siRNA and pcDNA3.1-FAM83D plasmids were provided by Shanghai GenePharma Pharmaceutical Technique Co., Ltd. (Shanghai, China).

MTT (3-[4,5-dimethylthiazol-2-yl]-2,5 diphenyl tetrazolium bromide) assays

Cells were seeded into a 96-well plate at a density of 1×10^4/well, and when the confluence reached 70%, 10 μL of MTT reagent (5 mg/mL, Sigma, USA) was added for incubation at 37°C for 4 h, and then the supernatant was discarded. The sediment was then washed in phosphate buffer solution (PBS) once, and to each well, 100 μL dimethylsulfoxide (DMSO) (Sigma, USA) was added, followed by incubation on a shaker for 10 min. Cells were subjected to the measurement of optical density at 490 nm in a microplate reader at 0, 24, 48 and 72 h after the cells were seeded. This experiment was conducted in triplicate, and the measurements were averaged as the final result.

Colony formation assays

Transfected cells in logarithmic phase were digested with trypsin and prepared as a single-cell suspension. After the cells were counted, 100 cells were seeded into a 6-well plate and cultured in 10 mL of complete medium for two weeks. The supernatant was discarded when the cell colonies became visible to the naked eye. Then, the cells were washed with PBS and fixed in methanol for 30 min. The cells were stained with Giemsa for 20 min and dried at room temperature. The colonies were then imaged and counted.

Transwell assays

Matrigel preserved at -80°C was dissolved at 4°C overnight, mixed with serum-free DMEM at a dilution of 1:8 and coated on the surface of a polycarbonate membrane (pore size: 8 μm), 50 μL/well, at room temperature for 4 h until the Matrigel coagulated. Glioma cells in each group were digested in trypsin, after which the cell density was adjusted to 10^5 cells/mL. Then, 200 μL of cell suspension was seeded into the upper Transwell chambers (BD Biosciences, USA), while 300 μL DMEM was added into the lower Transwell chambers. The Transwell chambers were then placed in an incubator (37°C, 5% CO_2). After 24 h, the liquid in the upper chambers was discarded and cells failing to pass through the membrane were removed with a wet cotton swab, and the remaining cells were fixed in methanol and stained in 0.1% crystal violet for 20 min. Stained cells in the Transwell chambers were rinsed in water and then PBS three times. The basal membrane was then collected to count the cells under the microscope. This experiment was conducted in triplicate.

Wound healing assays

After being transfected for 48 h, the cells were placed in serum-free medium with 1 μg/mL mitomycin C for 1 h. Then, a sterile 200 μL pipette tip was utilized to draw a line on the surface of the cell layer and the disrupted cells and debris was removed by rinsing the cells in serum-free medium. The wound was imaged under a microscope (Olympus, Japan) to record the positions of the cells. After being cultured in serum-free medium, the cells were imaged again. The widths of the wounds at 0 h and 48 h were recorded to calculate the wound healing rate of cells in each group. This experiment was conducted in triplicate.

Western blotting

Total proteins were extracted from the harvested tissues and cells, and the protein concentration was measured using a bicinchoninic acid (BCA) protein quantification kit (Thermo Fisher Scientific Inc., USA). Then, 30 μg of protein was added to loading buffer to separate the proteins by 10% sodium dodecyl sulfate–polyacrylamide gel electrophoresis (SDS–PAGE) and then they were transferred onto a polyvinylidene fluoride (PVDF) membrane using a semidry transfer (Bio–Rad, USA). The unoccupied sites were blocked by incubation in 5% nonfat milk for 1 h at room temperature. Proteins on the membrane were probed by being incubated with the primary rabbit polyclonal anti-FAM83D (ab236882, 1:500), anti-AKT (ab38449, 1:500), anti-p-AKT (ab38449, 1:500), anti-mTOR (ab2732, 1:2000), anti-p-mTOR (ab131538, 1:1000) and β-actin antibodies (ab8227, 1:1000, Abcam, UK) at 4°C overnight, which was then terminated by three washes in PBS at room temperature for 5 min/wash. The resulting immunoblots were further probed by incubation with goat polyclonal to rabbit horseradish peroxidase (HRP)-labeled secondary antibodies (32260, 1:10000, Thermo Fisher Scientific Inc., USA) at 37°C for 2 h, which was also terminated by three washes in PBS, 5 min/wash. The final immunoblots were visualized with chemiluminescence (ECL) reagent (Thermo Fisher Scientific Inc., USA), and the band intensity was determined and analyzed with ImageJ software, with β-actin as the loading control. The relative expression of target proteins was expressed as the ratio of the intensity of the target protein to that of β-actin.

Xenografted tumor models

A total of 12 BALB/c mice, 6 weeks of age, with an average weight of 17.5 ± 1.2 g, were provided by Shanghai Laboratory Animal Center, Chinese Academy of Sciences (CAS). For subcutaneous implantation, U87 cells in logarithmic phase in the siNC group and siFAM83D group were digested and 200 μL of a single-cell suspension containing 1×10^6 cells was then injected subcutaneously into the left shoulder, with 6 mice in each group. After injection, the nude mice were subjected to the following measurements: weight and length of the major and minor axis for calculating the volume of the tumor by using the formula: volume = (Length $_{major\ axis}$ × Length $^2_{minor\ axis}$) × 1/2. All nude mice were then sacrificed after 21 days followed by removal of the tumor tissues to record the weight of the tumors.

For intracranial implantation, U87 cells (1×10^5 cells/3 μL DMEM) transfected with siNC or siFAM83D were injected into the right striatum of the brain to a depth of 3 mm at a rate of 0.2 μL/min [17], with 6 mice in each group. For the analysis of survival, the mice were under periodic monitoring and were sacrificed when serious neurological symptoms appeared and/or an evident loss of weight (more than 20% of their body weight) occurred. Whole mouse brains were removed, fixed with 4% paraformaldehyde, and subjected to hematoxylin and eosin (H&E) staining. The tumor volume was then calculated using the same formula as in the subcutaneous model.

Immunohistochemistry

The excised tumors (each group contained 6 mice) were fixed in 10% methanol and embedded in paraffin. Paraffin blocks were then sliced into sections that were later deparaffinized and hydrated, followed by antigen retrieval. Sections were then placed in goat serum for blocking and incubated with a primary rabbit polyclonal anti-Ki67 antibody (ab15580, 1:300, Abcam, UK) for 2 h at room temperature, and the residual antibody was removed by absorbent paper. Sections were then rinsed in PBS on a shaker twice for 4 min/wash. The goat polyclonal to rabbit horseradish peroxidase (HRP)-labeled secondary antibody (32260, 1:10000, Thermo Fisher Scientific Inc., USA) was then dropped on the sections for incubation at room temperature for 45 min, followed by washes in PBS, with the residual liquid being discarded. Sections

were stained in hematoxylin for 5 min, dehydrated in ethanol, cleared in xylene twice (10 min for each), mounted by neutral balsam and sealed under coverslips for observation under the microscope.

Statistical analysis

All data were analyzed by SPSS 21.0 (SPSS, Inc., Chicago, IL, USA). Measurement data are expressed as the mean ± standard deviation (SD). Data among groups obtained from western blotting colony formation, migration, and invasion assays were compared by one-way analysis of variance (one-way ANOVA), followed by Tukey's *post hoc.* Two-way ANOVA was used to determine the significant differences in the results from the MTT assays. Differences in subcutaneous tumor volume from the nude mice between the siNC and siFAM83D groups were assessed by two-way ANOVA. Differences in the tumor weight from the nude mice between the siNC and siFAM83D groups were validated by using *t*-tests. $P < 0.05$ meant that the difference was statistically significant.

Results

FAM83D expression was upregulated in glioma cells and tissues

First, data derived from The Cancer Genome Atlas (TCGA) database revealed that GBM patients have a higher expression of FAM83D than normal controls (Fig. 1A). Subsequently, western blotting was performed to determine the expression of FAM83D in glioma tissues and cells (Fig. 1B-C). In comparison with normal tissues (0.19 ± 0.06), FAM83D expression in glioma tissues was increased and was much higher in patients with grade III-IV (1.02 ± 0.15) glioma (all $P < 0.05$). Glioma cell lines, including U87 (1.05 ± 0.12), U251 (1.08 ± 0.15), T98G (0.62 ± 0.08), SHG44 (0.83 ± 0.09) and U118 (0.89 ± 0.10), also presented higher expression of FAM83D than the normal cell line NHA (0.21 ± 0.05), while the highest expression was found in U87 and U251 cells, which were selected for the following experiments.

Overexpression of FAM83D activated the AKT/mTOR pathway

Western blotting was carried out to determine the expression of FAM83D and components of the AKT/mTOR pathway in U251 and U87 cells (Fig. 2). The expression of p-AKT/AKT and p-mTOR/mTOR in the siFAM83D group (U87 cells: FAM83D: 0.21 ± 0.04; p-AKT/AKT: 0.18 ± 0.03; p-mTOR/mTOR: 0.23 ± 0.04; U251 cells: FAM83D: 0.19 ± 0.04; p-AKT/AKT: 0.18 ± 0.03; p-mTOR/mTOR: 0.22 ± 0.04) and MK2206 group (U87 cells: FAM83D: 1.06 ± 0.13; p-AKT/AKT: 0.13 ± 0.03; p-mTOR/mTOR: 0.25 ± 0.05; U251 cells: FAM83D: 1.02 ± 0.12; p-AKT/AKT: 0.16 ± 0.04; p-mTOR/mTOR: 0.79 ± 0.08) was decreased as compared to the Mock group (U87 cells: FAM83D: 1.06 ± 0.15; p-AKT/AKT: 0.81 ± 0.09; p-mTOR/mTOR: 0.86 ± 0.08; U251 cells: FAM83D: 2.15 ± 0.21; p-AKT/AKT: 1.35 ± 0.12; p-mTOR/mTOR: 1.41 ± 0.15), while the FAM83D group had upregulation of FAM83D (U87 cells: 2.15 ± 0.26; U251 cells: 2.16 ± 0.21), p-AKT/AKT (U87 cells: 1.58 ± 0.16; U251: 1.35 ± 0.12) and p-mTOR/mTOR (U87 cells: 1.62 ± 0.15; U251: 1.41 ± 0.15; all $P < 0.05$). In addition, the expression of FAM83D in the FAM83D + MK2206 group (U87 cells: FAM83D: 2.18 ± 0.28; p-AKT/AKT: 0.82 ± 0.09; p-mTOR/mTOR: 0.87 ± 0.11; U251 cells: FAM83D: 2.18 ± 0.19; p-AKT/AKT: 0.75 ± 0.08; p-mTOR/mTOR: 0.84 ± 0.09) was not significantly different from that in the FAM83D group ($P > 0.05$), but the expression of p-AKT/AKT and p-mTOR/mTOR was lower in the FAM83D + MK2206 group than in the FAM83D group (all $P < 0.05$). Hence, silencing FAM83D inhibited the expression of components of the AKT/mTOR pathway.
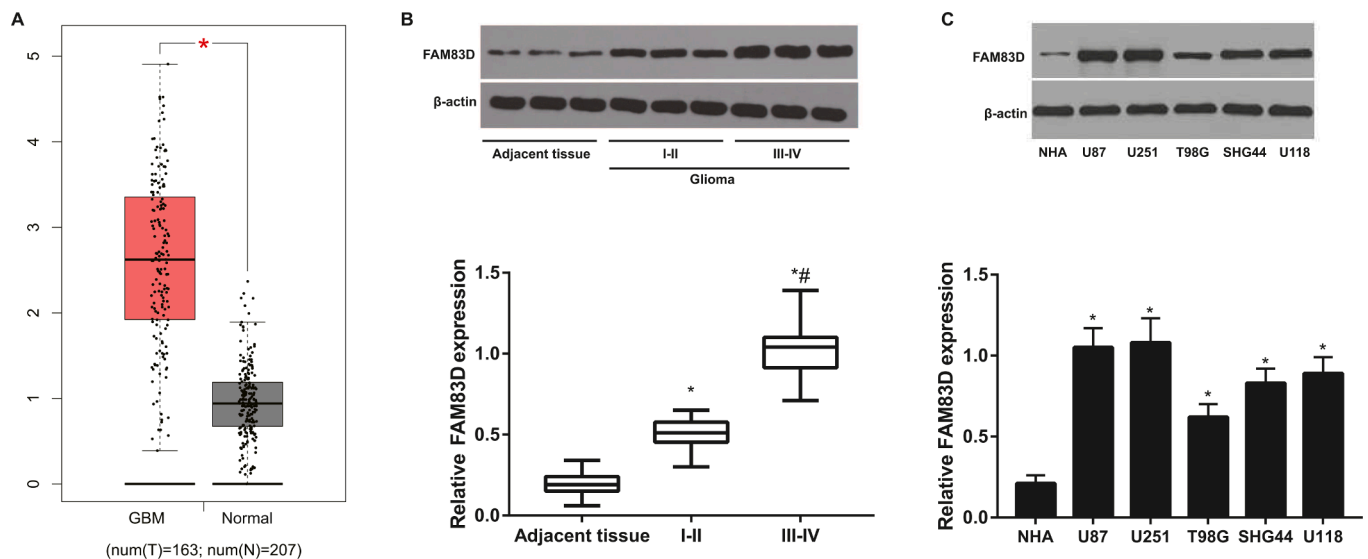
Fig. 1. Expression of FAM83D in glioma cells and tissues. A, TCGA database demonstrated that FAM83 was highly expressed in GBM patients; * $P < 0.05$ *vs.* normal tissues; B, Western blotting was conducted to determine the protein expression of FAM83D in glioma and adjacent tissues; * $P < 0.05$ *vs.* tumor-adjacent normal tissues; # $P < 0.05$ *vs.* glioma patients in grade I or II; C, Western blotting was conducted to determine the protein expression of FAM83D in glioma cell lines (U87, U251, T98G, SHG44 and U118) and normal human astrocytes (NHAs); * $P < 0.05$ *vs.* NHA cells.

FAM83D promoted the proliferation of glioma cells through the AKT/mTOR pathway

MTT assays and colony formation assays were carried out to determine the effect of FAM83D on the proliferation of U87 and U251 cells (Fig. 3). By comparison with the Mock group, cells in the siNC group showed no significant difference in cell proliferation or colony numbers ($P > 0.05$), while significant declines were observed in these two aspects in the siFAM83D group (colony numbers: U87 cells: 48.7±5.8; U251 cells: 45.7 ± 6.1) and MK2206 group (colony numbers: U87 cells: 47.3 ± 4.9; U251 cells: 44.3 ± 5.4; all $P < 0.05$). Nevertheless, the opposite changes were noted in the FAM83D group (colony numbers: U87 cells: 195.3 ± 21.5; U251 cells: 198.3 ± 18.7; all $P < 0.05$). In addition, when compared with the FAM83D group, cells in the FAM83D + MK2206 group showed significantly decreased cell proliferation and colony numbers (colony numbers: U87 cells: 115.7 ± 13.5; U251 cells: 114.3 ± 12.8; all $P < 0.05$), indicating that silencing FAM83D could inhibit the proliferation of glioma cells by inactivating the AKT/mTOR pathway.

FAM83D promoted the invasion and migration of glioma cells through the AKT/mTOR pathway

Transwell assays and wound healing tests were carried out to determine the invasive and migration abilities of U87 and U251 cells. As shown in Fig. 4, cells in the siFAM83D group showed significantly decreased invading cell numbers (U87 cells: 71.3 ± 8.5; U251 cells: 68.7 ± 6.5) and wound closure (U87 cells: 21.23 ± 3.58; U251 cells: 21.36 ± 2.58), while those in the FAM83D group (U87 cells: invasion: 252.3 ± 23.1; migration: 67.89 ± 8.52; U251 cells: invasion: 247.3 ± 26.7; migration: 76.58 ± 7.85) had significant enhancement in the above indicators compared with the Mock group (all $P < 0.05$). Furthermore, compared to the FAM83D group, cells in the FAM83D + MK2206 group also experienced sharp decreases in the invading cell numbers (U87: cells 154.3 ± 12.8; U251: 154.7 ± 16.8) and wound closure (U87 cells: 43.54 ± 5.06; U251 cells: 46.17 ± 5.14; all $P < 0.05$). Thus, silencing FAM83D could inhibit the AKT/mTOR pathway, which reduced the invasive and migration abilities of glioma cells.

Silencing FAM83D suppressed the growth of xenograft tumors in nude mice

To provide evidence that FAM83D regulated glioma growth *in vivo*, we established both subcutaneous and intracranial xenografted models of U87 cells in nude mice. In the subcutaneous model (Fig. 5A-D), in comparison with the siNC group, xenograft tumors in nude mice of the siFAM83D group grew much slower, with a great reduction in the weight of the tumors (tumor weight: siNC: 0.965 ± 0.087; siFAM83D: 0.426 ± 0.064; all $P < 0.05$).

Immunohistochemistry was conducted to determine the expression of Ki67 in the tumor tissues, and there was decreased positive expression of Ki67 in the siFAM83D group relative to the siNC group. In the intracranial model (Fig. 5E-G), Kaplan–Meier curves showed that mice in the siFAM83D group had longer survival times than those in the siNC group ($P < 0.05$). H&E staining of coronal brain sections showed that the average volume of the siNC tumors (36.45 ± 6.87 mm^3) was greater than that of the siFAM83D tumors (13.28 ± 3.24 mm^3, $P < 0.05$). Hence, silencing FAM83D could inhibit the *in vivo* growth of glioma cells.

Discussion

First, we found that FAM83D was upregulated in glioma tissues and cells, and a higher grade was associated with more evident upregulation of FAM83D. Similarly, Xuling Liu *et al.* reported that FAM83 was elevated in liver cancer, demonstrating a close association with the clinical stage and prognosis of patients [18]. Current studies have shown the amplification and overexpression of FAM83D in a variety of human cancers, including gastric cancer [19], colorectal cancer [10] and lung adenocarcinoma [20], which indicates that FAM83D is involved in tumorigenesis and cancer development.

FAM83D, also known as CHICA, was initially reported to interact with chromokinesin (KID) and is involved in the translocation of KID to the spindle body during mitosis to maintain the regular progression of mitosis [21]. It can also interact with other proteins in the spindle body, including DYNLL1 (dynein light chain 1) and HMMR, thus affecting the rotation and orientation of the spindle body [22]. Functional aberration of the spindle can lead to errors in chromosome separation and subsequent aneuploidy, as is often seen in advanced human cancers [23]. Therefore, FAM83D may act as an oncogene in the development and progression of various cancers, including glioma, by regulating mitosis.
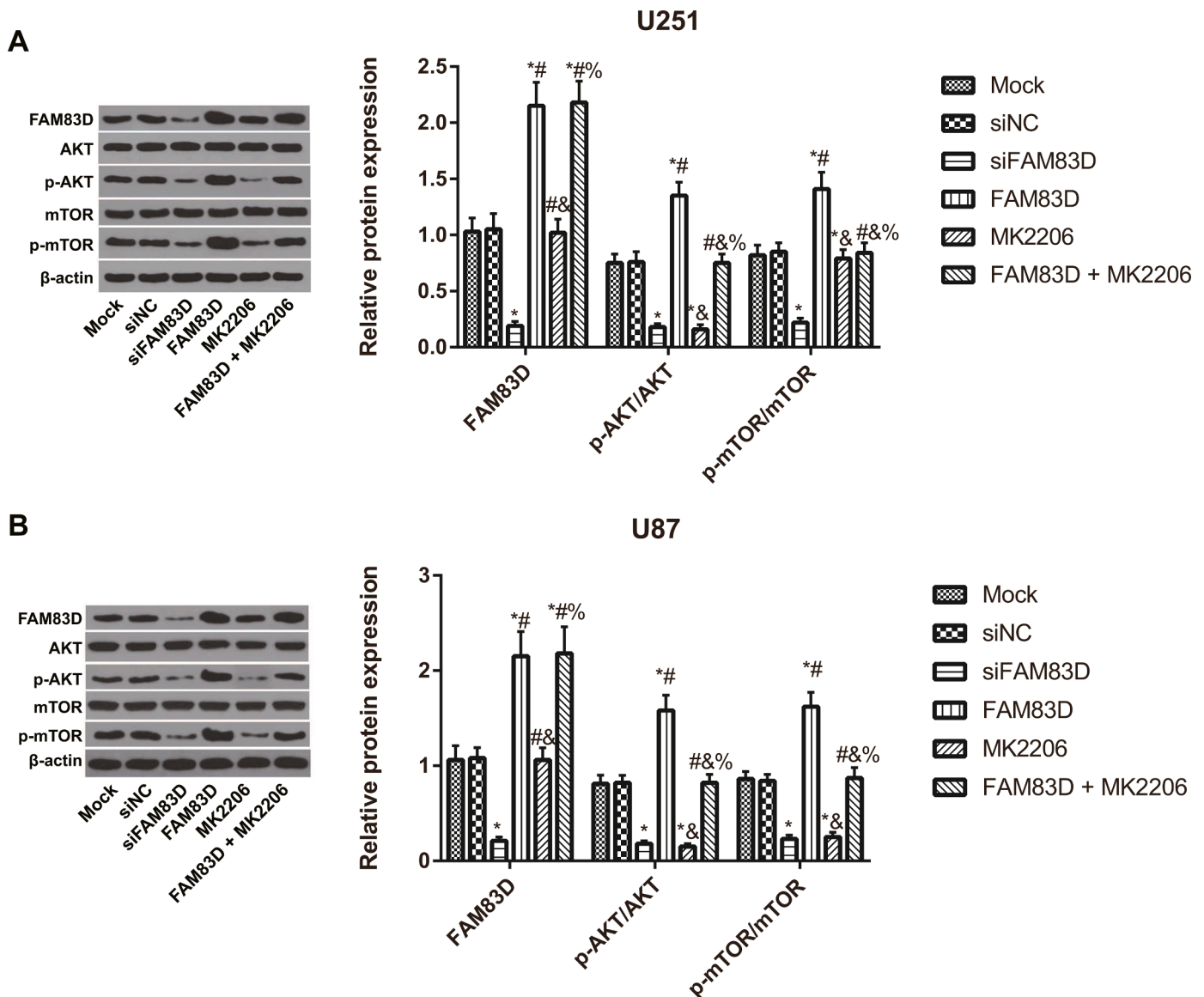
Fig. 2. Expression of FAM83D and the AKT/mTOR pathway in U251 and U87 cells. A-B, Western blotting was conducted to determine the protein expression of FAM83D, p-AKT/AKT and p-mTOR/mTOR in glioma U251 (A) and U87 (B) cell lines; * $P < 0.05$ *vs.* the Mock group; # $P < 0.05$ *vs.* the siFAM83D group; & $P < 0.05$ *vs.* the FAM83D group; % $P < 0.05$ *vs.* the MK2206 group.

Additionally, we performed a series of *in vitro* experiments to explore further the influence of FAM83D in glioma. Silencing FAM83D reduced the expression of p-AKT/AKT and p-mTOR/mTOR, while its overexpression caused the opposite changes, inactivating the AKT/mTOR signaling pathway in glioma by silencing FAM83D. Previous findings have confirmed the dysregulated expression of AKT/mTOR in glioma [24]. The expression of AKT was shown to be positively correlated with the malignancy of glioma, and inhibiting AKT could inhibit the proliferation and invasive abilities of glioma cells [25,26]. Additionally, mTOR is a central element in the evolutionarily conserved signaling pathway that regulates cell growth and metabolism, while aberrant mTOR signaling pathway activation contributes significantly to the initiation and development of glioma [27]. AKT harbors a PH domain that could bind to PIP3 to induce changes in the conformation of AKT, while PDK1 and PDK2 could bind to AKT to phosphorylate Thr308 and Ser473 to activate AKT [28,29]. Then, excessively activated AKT could continuously activate the mTOR pathway in glioma, and mTOR could trigger the expression of related genes to regulate the growth of tumor cells and accelerate the progression of glioma by integrating multiple

signals, including growth factors, amino acids and glucose [30,31].

Moreover, the activation of the AKT pathway also leads to an increase in the activity and expression of MMPs to mediate the degradation of type IV collagen in the basal membrane of the extracellular matrix, thereby promoting the outward infiltration, invasion and metastasis of glioma cells [32,33]. Likewise, Hongtao Zhu *et al.* reported that FAM83D, by activating the PI3K/AKT/mTOR pathway, could facilitate proliferation and invasion but inhibit autophagy in ovarian cancer cells [34]. Hence, inhibition of tumor progression by targeting AKT/mTOR is becoming a key approach to glioma gene therapy. MiR-495, as observed by Likun Yan *et al.*, could reduce the activity of the PTEN/P13K/AKT/mTOR pathway and inhibit the proliferation and metastasis of colorectal cancer cells by targeted downregulation of FAM83D [35]. Consistent with the above report, our data showed that silencing FAM83D may block the progression of glioma by inhibiting the activity of AKT/mTOR.

Tumor development is accompanied by abnormal cell proliferation, invasion and metastasis [36]. As revealed by our results, inhibiting FAM83D could limit the proliferation, invasion and migration abilities
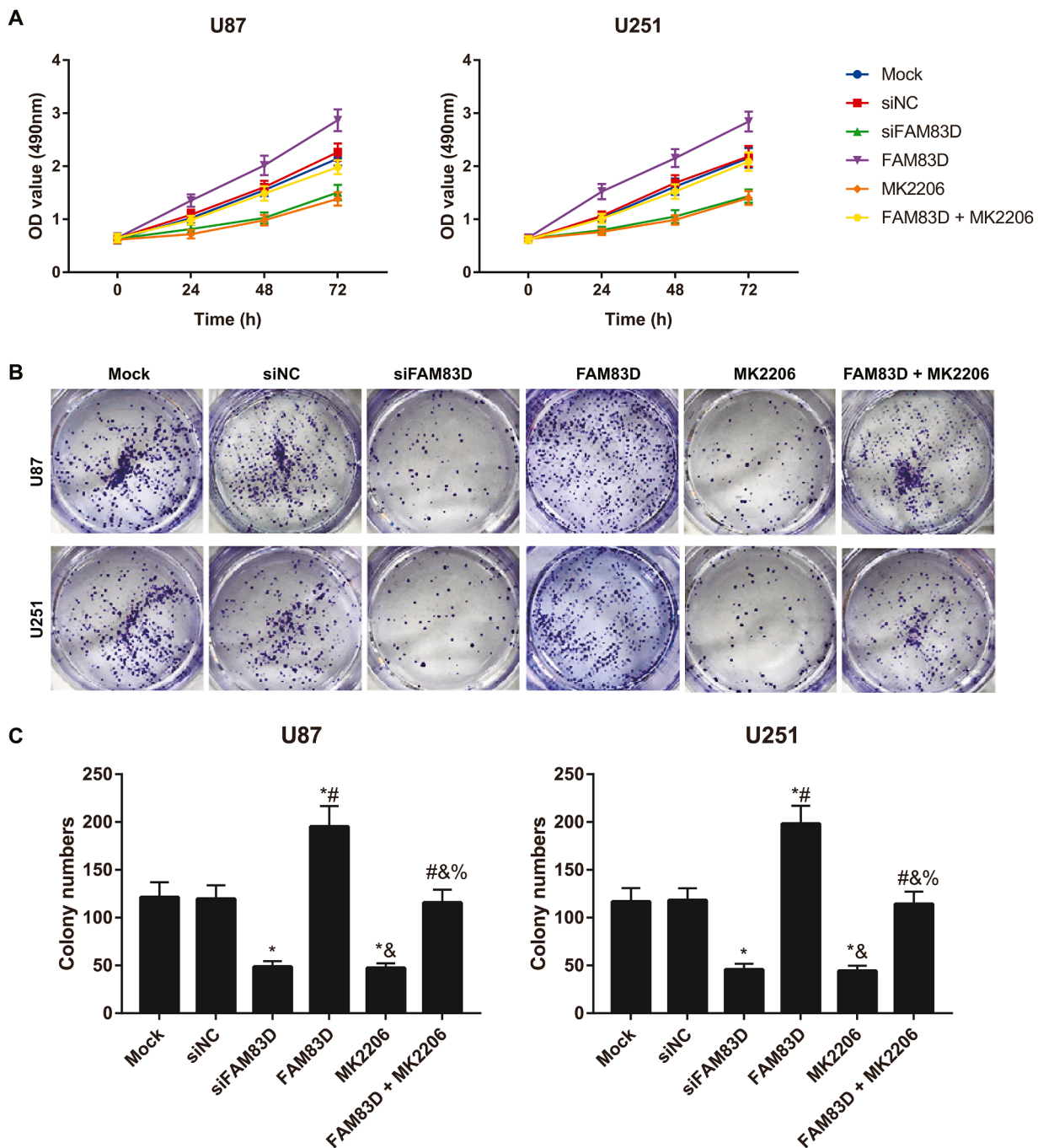
Fig. 3. Effect of the FAM83D-mediated AKT/mTOR pathway on the proliferation of glioma cells. A, MTT assays were conducted to evaluate the proliferation ability of U87 and U251 cells; B, Colony formation assays were conducted to determine the colony formation of U87 and U251 cells; C, Comparison of the colony numbers between U87 and U251 cells; * $P < 0.05$ *vs.* the Mock group; # $P < 0.05$ *vs.* the siFAM83D group; & $P < 0.05$ *vs.* the FAM83D group; % $P < 0.05$ *vs.* the MK2206 group.

of glioma cells, while overexpression resulted in the opposite changes. According to a previous study, knockout of FAM83D contributes to inhibition of the growth and EMT progression of esophageal squamous cancer cells by decreasing Akt/GSK-3β/Snail pathway activity [37]. According to Yuewen Chao *et al.*, Mst1 was noted to curb the proliferation abilities of glioma cells by inhibiting the AKT/mTOR pathway, suggesting that an inhibitor of AKT might be a new therapeutic approach to the treatment of malignant glioma [38]. In addition, MK-2206, as a novel AKT inhibitor, specifically inhibited the activation of PI3K/AKT [39], which was shown to reverse the positive effect of FAM83D on the growth and metastasis of glioma cells in our study. Relevant studies have

reported that MK-2206 could induce the autophagy and apoptosis of glioma cells, manifesting potent antitumor activity [40]. Furthermore, Yin C *et al.* found that MK-2206 could abolish the promoting effect of FAM83D on the proliferation, invasion and EMT process in NSCLC [14]. Taken together, these results suggest that silencing FAM83D could be a treatment approach by restricting the proliferation, invasion and migration of glioma cells and inhibiting the AKT/mTOR pathway. However, one gene can regulate multiple pathways. A limitation of this study was the fact that no other pathways were taken into consideration, compromising the interpretation of the relationship between FAM83D, the AKT/mTOR pathway, and the experimental results. Further analyses
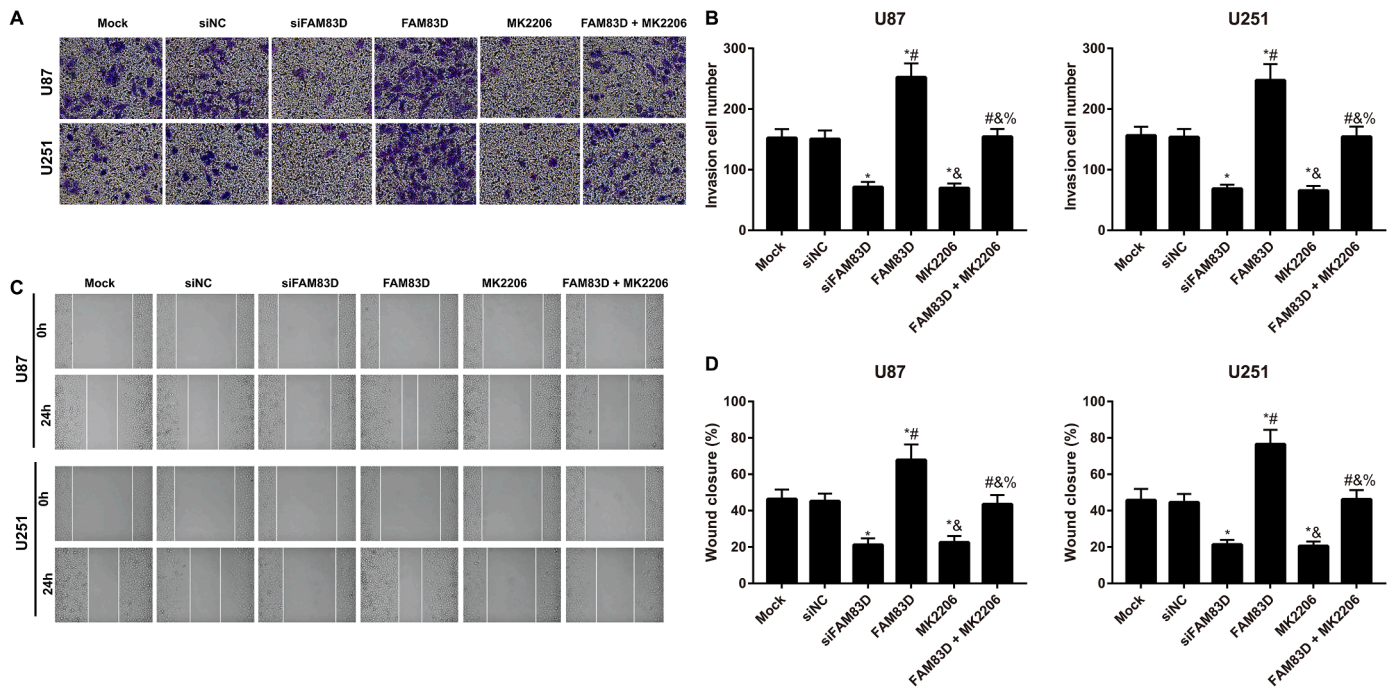
Fig. 4. Effect of the FAM83D-mediated AKT/mTOR pathway on the invasion and migration abilities of glioma cells. A, Transwell assays were conducted to determine the invasive abilities of U87 and U251 cells; B, Comparison of the invaded cell numbers between U87 cells and U251 cells; C, Wound healing tests were conducted to determine the migration abilities of U87 and U251 cells; B, Comparison of the wound closure between U87 cells and U251 cells; * $P < 0.05$ *vs.* the Mock group; # $P < 0.05$ *vs.* the siFAM83D group; & $P < 0.05$ *vs.* the FAM83D group; % $P < 0.05$ *vs.* the MK2206 group.
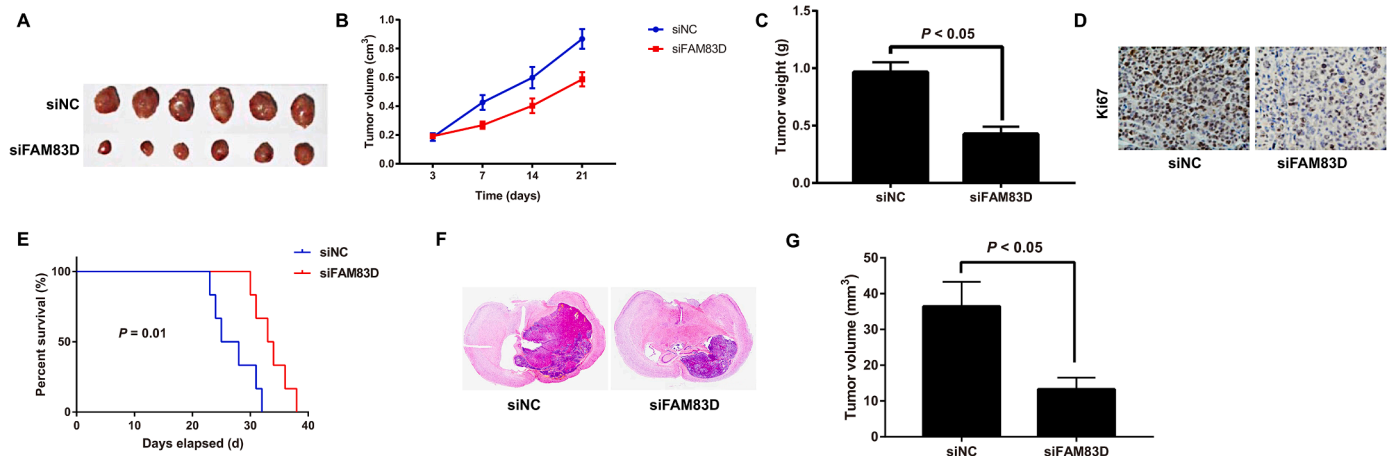

Fig. 5. Effect of silencing FAM83D on the growth of xenograft tumors in subcutaneous (A-D) and intracranial (E-G) mouse models. A, Gross specimens of xenograft tumors of nude mice; B, Growth curve of xenograft tumors in nude mice; C, Comparison of the weight of xenograft tumors among groups; D, Immunohistochemistry analysis of Ki67 protein levels in xenograft tumor tissues; E, Mouse survival shown in Kaplan–Meier curves; F, Representative images of H&E staining of mouse brain sections; G, The tumor volume in the siNC and siFAM83D groups were analyzed.

are needed to understand this regulatory mechanism in more detail.

In conclusion, we identified elevated expression of FAM83D in glioma. Furthermore, silencing FAM83D suppressed the proliferation, invasion and migration of glioma cells through inhibition of the AKT/mTOR pathway, providing a novel strategy for targeted therapy of glioma.

Author contribution

Xia Li: Manuscript writing; **Cui Sun**: Data collection; **Jing Chen**: Literature search; **Ji-Fen Ma**: Experiment conduction; **Yi-Heng Pan**: Validation and supervision; **All authors**: Manuscript review and technical correction.

Conflict of Interest Statement

The authors declare that they have no competing interests.

References

[1] C Fearon, T Loftus, AL Byrne, J Heffernan, M Cooney, C Heeney, et al., Impact of the 2016 World Health Organization Classification of Tumours of the Central Nervous System: an Irish experience, Irish journal of medical science 189 (2020) 799–803.

[2] EG Van Meir, CG Hadjipanayis, AD Norden, HK Shu, PY Wen, JJ. Olson, Exciting new advances in neuro-oncology: the avenue to a cure for malignant glioma, CA: a cancer journal for clinicians 60 (2010) 166–193.

[3] P Hainaut, A. Plymoth, Targeting the hallmarks of cancer: towards a rational approach to next-generation cancer therapy, Current opinion in oncology 25 (2013) 50–51.

[4] K Lenting, R Verhaak, M Ter Laan, P Wesseling, W Leenders, Glioma: experimental models and reality, Acta neuropathologica 133 (2017) 263–282.

[5] NA Bush, SM Chang, MS. Berger, Current and future strategies for treatment of glioma, Neurosurgical review 40 (2017) 1–14.

[6] M Madany, TM Thomas, L Edwards, JS. Yu, Immunobiology and immunotherapeutic targeting of glioma stem cells, Advances in experimental medicine and biology 853 (2015) 139–166.

[7] L Jiang, P Mao, L Song, J Wu, J Huang, C Lin, et al., miR-182 as a prognostic marker for glioma progression and patient survival, The American journal of pathology 177 (2010) 29–38.

[8] J Bai, PJ Mei, H Liu, C Li, W Li, YP Wu, et al., BRG1 expression is increased in human glioma and controls glioma cell proliferation, migration and invasion in vitro, Journal of cancer research and clinical oncology 138 (2012) 991–998.

[9] Z Wang, Y Liu, P Zhang, W Zhang, W Wang, K Curr, et al., FAM83D promotes cell proliferation and motility by downregulating tumor suppressor gene FBXW7, Oncotarget 4 (2013) 2476–2486.

[10] Y Mu, H Zou, B Chen, Y Fan, S. Luo, FAM83D knockdown regulates proliferation, migration and invasion of colorectal cancer through inhibiting FBXW7/Notch-1 signalling pathway, Biomedicine & pharmacotherapy = Biomedecine & pharmacotherapie 90 (2017) 548–554.

[11] F Janku, JJ Wheler, SN Westin, SL Moulder, A Naing, AM Tsimberidou, et al., PI3K/AKT/mTOR inhibitors in patients with breast and gynecologic malignancies harboring PIK3CA mutations, Journal of clinical oncology: official journal of the American Society of Clinical Oncology 30 (2012) 777–782.

[12] AS. Alzahrani, PI3K/Akt/mTOR inhibitors in cancer: At the bench and bedside, Seminars in cancer biology 59 (2019) 125–132.

[13] X Li, C Wu, N Chen, H Gu, A Yen, L Cao, et al., PI3K/Akt/mTOR signaling pathway and targeted therapy for glioblastoma, Oncotarget 7 (2016) 33440–33450.

[14] C Yin, X Lin, Y Wang, X Liu, Y Xiao, J Liu, et al., FAM83D promotes epithelial-mesenchymal transition, invasion and cisplatin resistance through regulating the AKT/mTOR pathway in non-small-cell lung cancer, Cellular oncology 43 (2020) 395–407.

[15] In: th, editor. Guide for the Care and Use of Laboratory Animals. Washington (DC) 2011.

[16] DN Louis, A Perry, G Reifenberger, A von Deimling, D Figarella-Branger, WK Cavenee, et al., The 2016 World Health Organization Classification of Tumors of the Central Nervous System: a summary, Acta neuropathologica 131 (2016) 803–820.

[17] Z Zhu, K Li, D Xu, Y Liu, H Tang, Q Xie, et al., ZFX regulates glioma cell proliferation and survival in vitro and in vivo, Journal of neuro-oncology 112 (2013) 17–25.

[18] X Liu, H Gao, J Zhang, D. Xue, FAM83D is associated with gender, AJCC stage, overall survival and disease-free survival in hepatocellular carcinoma, Bioscience reports (2019) 39.

[19] M Huang, X Ma, H Shi, L Hu, Z Fan, L Pang, et al., FAM83D, a microtubule-associated protein, promotes tumor growth and progression of human gastric cancer, Oncotarget 8 (2017) 74479–74493.

[20] R Shi, J Sun, Q Sun, Q Zhang, W Xia, G Dong, et al., Upregulation of FAM83D promotes malignant phenotypes of lung adenocarcinoma by regulating cell cycle, American journal of cancer research 6 (2016) 2587–2598.

[21] A Santamaria, S Nagel, HHW Sillje, EA. Nigg, The spindle protein CHICA mediates localization of the chromokinesin Kid to the mitotic spindle, Current biology: CB 18 (2008) 723–729.

[22] AK Dunsch, D Hammond, J Lloyd, L Schermelleh, U Gruneberg, FA. Barr, Dynein light chain 1 and a spindle-associated adaptor promote dynein asymmetry and spindle orientation, The Journal of cell biology 198 (2012) 1039–1054.

[23] PJ Walian, B Hang, JH. Mao, Prognostic significance of FAM83D gene expression across human cancer types, Oncotarget 7 (2016) 3332–3340.

[24] M Chen, X Yin, C Lu, X Chen, H Ba, J Cai, et al., Mahanine induces apoptosis, cell cycle arrest, inhibition of cell migration, invasion and PI3K/AKT/mTOR signalling pathway in glioma cells and inhibits tumor growth in vivo, Chemico-biological interactions 299 (2019) 1–7.

[25] QW Fan, WA. Weiss, Autophagy and Akt promote survival in glioma, Autophagy 7 (2011) 536–538.

[26] E Chautard, ZG Ouedraogo, J Biau, P. Verrelle, Role of Akt in human malignant glioma: from oncogenesis to tumor aggressiveness, Journal of neuro-oncology 117 (2014) 205–215.

[27] B Ren, L Wang, Y Nan, T Liu, L Zhao, H Ma, et al., RAB1A regulates glioma cellular proliferation and invasion via the mTOR signaling pathway and epithelial-mesenchymal transition, Future oncology 17 (2021) 3203–3216.

[28] N Berndt, H Yang, B Trinczek, S Betzi, Z Zhang, B Wu, et al., The Akt activation inhibitor TCN-P inhibits Akt phosphorylation by binding to the PH domain of Akt and blocking its recruitment to the plasma membrane, Cell death and differentiation 17 (2010) 1795–1804.

[29] I Nepstad, KJ Hatfield, IS Gronningsaeter, H. Reikvam, The PI3K-Akt-mTOR Signaling Pathway in Human Acute Myeloid Leukemia (AML) Cells, International journal of molecular sciences 21 (2020).

[30] SY Shin, KS Lee, YK Choi, HJ Lim, HG Lee, Y Lim, et al., The antipsychotic agent chlorpromazine induces autophagic cell death by inhibiting the Akt/mTOR pathway in human U-87MG glioma cells, Carcinogenesis 34 (2013) 2080–2089.

[31] N Koul, V Sharma, D Dixit, S Ghosh, E. Sen, Bicyclic triterpenoid Iripallidal induces apoptosis and inhibits Akt/mTOR pathway in glioma cells, BMC cancer 10 (2010) 328.

[32] Y Bi, H Li, D Yi, Y Sun, Y Bai, S Zhong, et al., Cordycepin Augments the Chemosensitivity of Human Glioma Cells to Temozolomide by Activating AMPK and Inhibiting the AKT Signaling Pathway, Molecular pharmaceutics 15 (2018) 4912–4925.

[33] Y Yu, X Fu, Q Ran, K Yang, Y Wen, H Li, et al., Globularifolin exerts anticancer effects on glioma U87 cells through inhibition of Akt/mTOR and MEK/ERK signaling pathways in vitro and inhibits tumor growth in vivo, Biochimie 142 (2017) 144–151.

[34] H Zhu, S Diao, V Lim, L Hu, J. Hu, FAM83D inhibits autophagy and promotes proliferation and invasion of ovarian cancer cells via PI3K/AKT/mTOR pathway, Acta biochimica et biophysica Sinica 51 (2019) 509–516.

[35] L Yan, J Yao, J. Qiu, miRNA-495 suppresses proliferation and migration of colorectal cancer cells by targeting FAM83D, Biomedicine & pharmacotherapy = Biomedecine & pharmacotherapie 96 (2017) 974–981.

[36] L Cao, F Wang, S Li, X Wang, D Huang, R. Jiang, PIM1 kinase promotes cell proliferation, metastasis and tumor growth of lung adenocarcinoma by potentiating the c-MET signaling pathway, Cancer letters 444 (2019) 116–126.

[37] YQ Hua, K Zhang, J Sheng, ZY Ning, Y Li, WD Shi, et al., Fam83D promotes tumorigenesis and gemcitabine resistance of pancreatic adenocarcinoma through the Wnt/beta-catenin pathway, Life sciences (2021) 119205.

[38] Y Chao, Y Wang, X Liu, P Ma, Y Shi, J Gao, et al., Mst1 regulates glioma cell proliferation via the AKT/mTOR signaling pathway, Journal of neuro-oncology 121 (2015) 279–288.

[39] R Liu, D Liu, E Trink, E Bojdani, G Ning, M. Xing, The Akt-specific inhibitor MK2206 selectively inhibits thyroid cancer cells harboring mutations that can activate the PI3K/Akt pathway, The Journal of clinical endocrinology and metabolism 96 (2011) E577–E585.

[40] Y Cheng, X Ren, Y Zhang, R Patel, A Sharma, H Wu, et al., eEF-2 kinase dictates cross-talk between autophagy and apoptosis induced by Akt Inhibition, thereby modulating cytotoxicity of novel Akt inhibitor MK-2206, Cancer research 71 (2011) 2654–2663.